

Dielectric omnidirectional visible reflector

M. Deopura, C. K. Ullal, B. Temelkuran, and Y. Fink

Department of Material Science and Engineering, Massachusetts Institute of Technology, Cambridge, Massachusetts 02139

Received January 31, 2001

We demonstrate the fabrication of an all-dielectric omnidirectional mirror for visible frequencies. The dielectric reflector consists of a stack of 19 alternating layers of tin (IV) sulfide and silica. Using a combination of thermal evaporation (for tin sulfide) and thick electron-beam evaporation (for silica), we have achieved a refractive-index contrast of 2.6/1.46, one of the highest refractive-index contrasts demonstrated in one-dimensional photonic bandgap systems designed for the visible frequency range. The tin sulfide–silica material system developed allowed the formation of a broadband visible reflector with an omnidirectional range greater than 10%. Possible applications of the system include efficient reflectors, high-frequency waveguides for communications and power delivery, and high- Q cavities. © 2001 Optical Society of America

OCIS codes: 300.6550, 140.7300, 310.6860.

Low-loss periodic dielectric structures called photonic crystals provide a mechanism for the efficient control of electromagnetic energy.^{1–3} Owing to its periodic dielectric structure, a dielectric crystal with a complete three-dimensional photonic bandgap can restrict light from propagation regardless of the direction of the wave vector for a specified frequency range and all polarizations. A considerable effort is under way to make three-dimensional photonic crystals at visible frequencies by use of a variety of techniques that rely on self-assembly or nanofabrication.^{4,5}

Creating structures with a photonic bandgap in the visible regime requires in most cases a characteristic feature size of the order of 100 nm. This requirement renders the fabrication of a structure with a complete photonic bandgap in the visible regime complex and costly.

The complications associated with three-dimensional photonic crystals have led to the pursuit of alternative strategies that employ structures that have incomplete bandgaps but are nevertheless much simpler to fabricate. In these structures electromagnetic energy confinement is achieved by the geometry of the cavity and the refractive index of the confining medium. An example of such a structure is the omnidirectionally reflecting,^{6–8} one-dimensional photonic crystal. This simple structure can be shaped to confine light in cavities or in waveguides.

The first dielectric omnidirectional reflector fabricated with a polystyrene–tellurium material system was tuned to reflect light in the infrared frequency.⁷ Here we extend the previously presented work and develop a new tin (IV) sulfide–silica material system that operates in the 600–800-nm wavelength range.

High refractive-index contrast is essential to the formation of large photonic bandgaps.⁹ However, in the visible frequency range, the lower values of electronic and ionic polarizability lead to an inherently low refractive-index value for most materials. Here, tin sulfide has been chosen as the high-refractive-index material ($n_b \sim 3.0$ at 600 nm for a bulk crystal¹⁰). From an extensive list of materials, tin sulfide seems to have the highest refractive index in the visible frequency range while at the same time

being optically low loss. Tin sulfide exhibits very low absorption below its characteristic 2.2-eV (590-nm) band edge.¹¹ Also, tin sulfide is easily amenable to thin-film deposition.¹² Recently, the high refractive index of tin sulfide was used to make inverted opal structure photonic crystal films for use in the visible regime.¹³ Here, silica ($n \sim 1.46$) has been chosen as the low-refractive-index material, as it has been extensively studied and used in the past to make thin films.

The tin (IV) sulfide–silica structure used to construct the omnidirectional reflector is depicted in Fig. 1. The structure profile describes layer thicknesses $h_1 = 60$ nm and $h_2 = 110$ nm and refractive indices $n_1 = 2.6$ and $n_2 = 1.46$ for tin sulfide and silica, respectively. A refractive index of $n_1 = 2.6$ for thin-film tin sulfide (as opposed to a refractive index of $n_b = 3.0$ for the bulk crystal), as measured according to standard techniques, has been used.¹⁴ A lower value of the refractive index in thin films than in the bulk crystal is usually observed.¹⁵ The band structure⁷ of the tin sulfide–silica system is presented

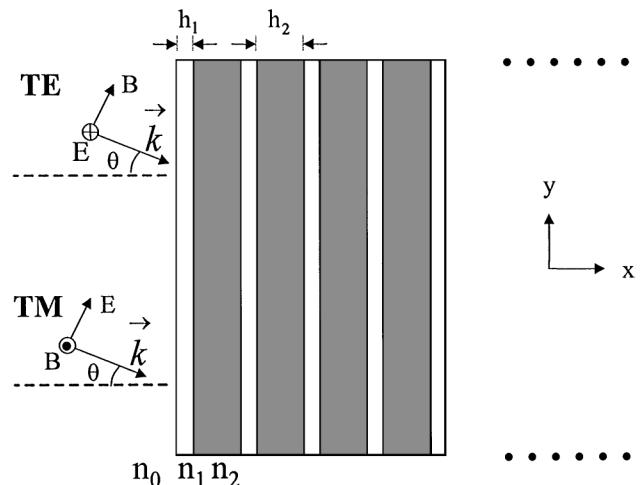


Fig. 1. Schematic of the multilayer system, showing the layer parameters (n_α and h_α are the index of refraction and the thickness of layer α , respectively), the incident wave vector \mathbf{k} , and the electromagnetic mode convention. \mathbf{E} and \mathbf{B} are the electric and magnetic fields, respectively.

in Fig. 2. The theoretically calculated values of ω_h and ω_l that define the omnidirectional band edges⁷ of the tin sulfide–silica system correspond to 630 and 710 nm. The characteristic dimensionless parameter $\eta = 2(\omega_h - \omega_l)/(\omega_h + \omega_l)$, which quantifies the extent of the omnidirectional range, has a value of $\eta \sim 13\%$ of our system.

When constructing an omnidirectional reflector for the visible frequencies, one faces a number of challenges. Very thin layers (individual layers of ~ 100 nm) need to be deposited for fabrication of these dielectric structures. (At infrared frequencies the layer thickness is ~ 1 μm .) The lower dielectric contrast available at optical frequencies requires that a large number of layers be deposited for high reflectivity values and a stop band to be achieved. Another challenge is to control surface roughness to an acceptable level ($\sim 1\%$) to minimize scattering loss and develop a process so that the materials conform mechanically without high stress buildup in the layers or delamination.

To fabricate 19 alternating layers of tin sulfide–silica structure, we deposited the two materials sequentially, using separate vacuum-deposition chambers. The tin sulfide (99.5%; Strem Chemicals) was deposited by a thermal evaporator (CVC) at 10^{-6} Torr and 10 A to yield a 80 ± 5 -nm-thick layer on a 22-mm square glass substrate (VWR glass coverslip). The layer thickness and deposition rate were monitored *in situ* with a crystal-thickness monitor (Sycon STM100). To verify the stoichiometry of the tin sulfide thin film, we characterized a single layer (250 nm) of the vacuum-deposited material, using Rutherford backscattering (RBS). In Fig. 3, the experimental profile of the RBS spectrum is presented, and it is in good agreement with the theoretically predicted profile for $\text{SnS}_{1.85}$. The RBS spectrum suggests a deviation from stoichiometry for the thin film; however, the deviation is very small to affect the optical properties significantly, as can be seen from the reflectivity measurements of the multilayer films. The silica was vacuum deposited by use of an electron-beam evaporator (NRC; 119) at 5×10^{-7} Torr at power levels of 10 kV and 0.05 kA to produce a 115 ± 10 -nm-thick layer. The layer thickness and deposition were monitored *in situ* by a built-in crystal monitor (Filtech). The 19-layer structure was characterized by cross-sectional scanning electron microscopy (with a field emission gun scanning electron microscope; JOEL), and the micrograph is presented in Fig. 4. The rms surface roughness measured with a profilometer was ~ 30 nm (thickness of the 19-layer structure, ~ 2 μm).

Several interesting observations are made based on looking at the mirror with the naked eye. The thin-film mirror has a golden appearance in white light, both at normal incidence and at oblique angles of incidence. When the mirror is held against white light, it allows blue-green light to be transmitted through it.

The optical response of the dielectric mirror has been designed to have high reflectivity in the 600–800-nm region for any angle of incidence (in the experiment we

measured from 0 to 70°). The response was measured with an ultraviolet–visible–near infrared spectrophotometer (Cary 500; Varian) fitted with a polarizer. Normal-incidence reflectivity measurements were made with a spectral reflectance accessory, and the

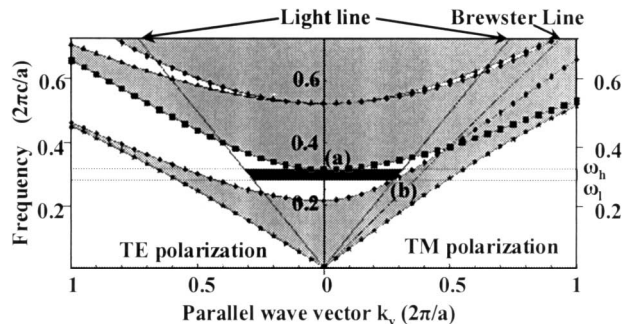


Fig. 2. Projected band structure of a multilayer film, together with the light line, showing an omnidirectional reflectance range in the first harmonic. Propagating states, light gray; evanescent states, white; omnidirectional reflectance range, black. The film parameters are $n_1 = 2.6$ and $n_2 = 1.46$, with thickness ratio $h_2/h_1 = 115/80$ for the tin sulfide–silica system.

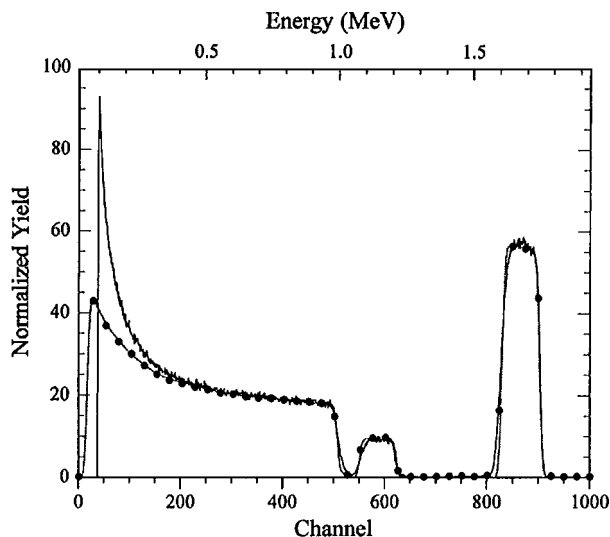


Fig. 3. RBS spectrum (curve with circles) of a 250-nm-thick layer of tin (IV) sulfide compared with a simulated spectrum (solid curve) of $\text{SnS}_{1.85}$.

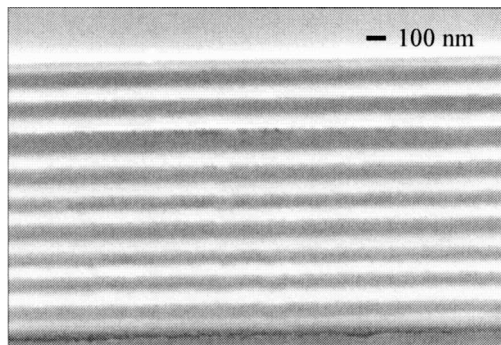


Fig. 4. Cross-sectional scanning electron microscope micrograph of the 19-layer tin sulfide–silica multilayer structure. The bright regions correspond to tin sulfide. The dark regions correspond to silica.

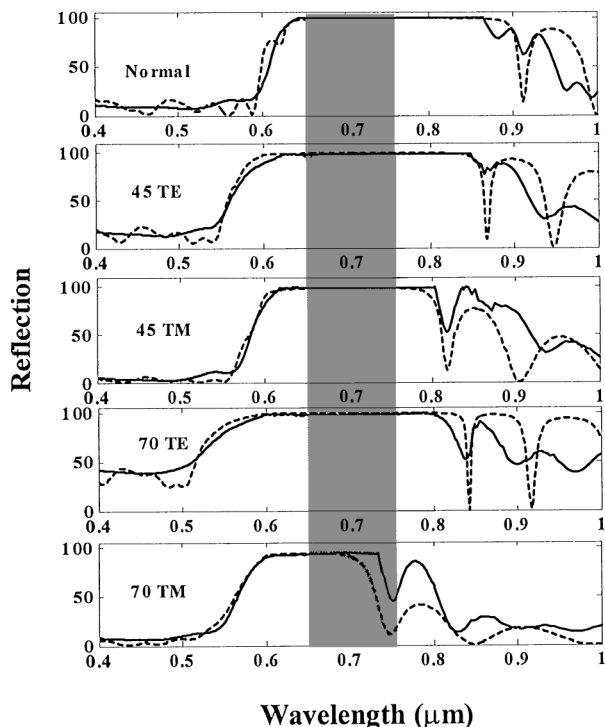


Fig. 5. Calculated (dashed traces) and measured (solid traces) reflectance spectra as a function of wavelength for TM and TE modes at normal, 45°, and 70° angles of incidence, showing an omnidirectional reflectivity band. A computer-generated color spectrum shows the visible colors ranging from 400 to 780 nm. The semitransparent red region shows the experimentally observed omnidirectional bandgap.

oblique angle measurements were made with a variable-angle reflectivity stage. A freshly evaporated aluminum mirror was used as the background for the reflectance measurements.

We observed very good agreement between the calculated¹⁶ (dashed traces) and measured (solid traces) reflectance spectra at normal, 45°, and 70° for the TE and TM modes, as shown in Fig. 5. The measured spectra from the spectrometer (for all the different angles and both polarizations) were corrected for absolute reflectivity values by use of a single-frequency He–Ne laser (632-nm) measurement.¹⁷ The regimes of high-reflectivity overlap form the omnidirectional band marked in Fig. 5. The experimental values of ω_h 640 nm and of ω_l 730 nm (as can be inspected visually from the reflectivity curves) compare well with the theoretically predicted values of ω_h 630 nm and ω_l 710 nm for the infinite-layer structure.

Finally, a demonstration of an omnidirectional visible mirror is presented. The materials and processes were chosen for their low cost and applicability to large area coverage. Optically, the mirror has a golden appearance and omnidirectional reflectivity for a broad range of visible frequencies and at the same time is low loss. The tin sulfide–silica material system has opened up a vast number of avenues for both research and practical applications. The visible mirror can potentially be used for high-frequency communications waveguiding (as an all-dielectric

coaxial cable¹⁸), whereas up to now the operation of material systems had been restricted to frequencies in the infrared. The omnidirectional mirror can provide reflection calibration standards for all angles in experimental optics, as it combines the properties of low loss and omnidirectionality. Another use of an omnidirectional mirror could be in fabrication laser cavities to get very low threshold lasers. A vast number of other potential applications exist. Besides these applications, there is also the truly unique aesthetic appeal of being able to perceive a reflection from a low-loss omnidirectional structure.

This work was supported by Nanovation Technologies. We acknowledge useful discussions with M. Bawendi, K. Broderick, J. D. Joannopoulos, and E. L. Thomas. M. Deopura's e-mail address is deopura@mit.edu.

References

1. E. Yablonovitch, *Phys. Rev. Lett.* **58**, 2059 (1987).
2. S. John, *Phys. Rev. Lett.* **58**, 2486 (1987).
3. J. D. Joannopoulos, R. Meade, and J. N. Winn, *Photonic Crystals: Molding the Flow of Light* (Princeton U. Press, Princeton, N.J., 1995).
4. S. Noda, *Physica B* **279**, 142 (2000).
5. S. Y. Lin and J. G. Fleming, *J. Lightwave Technol.* **24**, 49 (1999).
6. J. N. Winn, Y. Fink, S. Fan, and J. D. Joannopoulos, *Opt. Lett.* **23**, 1573 (1998).
7. Y. Fink, J. N. Winn, S. Fan, C. Chen, J. Michel, J. D. Joannopoulos, and E. L. Thomas, *Science* **282**, 1679 (1998).
8. D. N. Chigrin, A. V. Lavrinenko, D. A. Yarotsky, and S. V. Gaponenko, *J. Lightwave Technol.* **17**, 2018 (1999).
9. For an omnidirectional structure there exists an optimum value of $n = 1.44$ for the low-refractive-index layer. For the high-refractive-index material a minimum value of $n = 2.2$ is required for omnidirectionality.
10. S. Mandalidis, J. A. Kalomiro, K. Kambas, and A. N. Anagnostopoulos, *J. Mater. Sci.* **31**, 5975 (1996).
11. P. A. Lee, G. Said, R. Davis, and T. H. Lim, *J. Phys. Chem. Solids* **30**, 2719 (1989).
12. K. Kawano, R. Nakata, and M. Sumita, *J. Phys. D* **22**, 136 (1989).
13. M. Müller, R. Zentel, T. Maka, S. G. Romanov, and C. M. Sotomayor Torres, *Adv. Mater.* **12**, 20 (2000).
14. E. D. Palik, ed., *Handbook of Optical Constants of Solids* (Academic, Boston, 1999), Vol. II, Chap. 3.
15. A common example of this is seen in titania (TiO_2), in which the bulk crystal refractive-index value is $n \sim 2.8$, whereas the thin-film refractive-index value is $n \sim 2.3$.
16. The calculations were done with the transfer matrix method described by F. Abeles, *Ann. Phys.* **5**, 706 (1950), with the film parameters.
17. The absolute reflectivity measurement was made with a 50/50 beam splitter that split the laser beam coming from the source. One of the split beams was focused directly into a powermeter, while the other split beam was focused into an identical detector after reflection from the mirror. The comparison of the power measured by the two detectors gave the absolute reflectivity value. Measurements were made for all angles at both polarizations.
18. M. Ibanescu, Y. Fink, S. Fan, E. L. Thomas, and J. D. Joannopoulos, *Science* **289**, 415 (2000).